Remote Sens. **2015**, *7*, 12986-13004; doi:10.3390/rs71012986

OPEN ACCESS

remote sensing

ISSN 2072-4292

www.mdpi.com/journal/remotesensing

Article

Frequency of Low Clouds in Taiwan Retrieved from MODIS Data and Its Relation to Cloud Forest Occurrence

Boris Thies [1,*], Alexander Groos [1], Martin Schulz [1], Ching-Feng Li [2], Shih-Chieh Chang [3] and Jörg Bendix [1]

[1] Faculty of Geography, Philipps-Universität Marburg, Deutschhausstrasse 12, 35032 Marburg, Germany; E-Mails: mail@alexandergroos.de (A.G); martin.schulz@staff.uni-marburg.de (M.S.); bendix@mailer.uni-marburg.de (J.B.)

[2] Department of Botany and Zoology, Masaryk University, Kotlářská 2, CZ-61137 Brno, Czech Republic; E-Mail: chingfeng.li@gmail.com

[3] Department of Natural Resources and Environmental Studies, National Dong Hwa University, 974 Hualien, Taiwan; E-Mail: scchang@mail.ndhu.edu.tw

* Author to whom correspondence should be addressed; E-Mail: thies@staff.uni-marburg.de; Tel.: +49-6421-282-5910; Fax: +49-6421-282-4833.

Academic Editors: Randolph Wynne and Prasad S. Thenkabail

Received: 3 March 2015 / Accepted: 26 September 2015 / Published: 30 September 2015

Abstract: The relationship between satellite-derived low cloud frequency and the occurrence of tropical montane cloud forest (TMCF) in Taiwan was investigated. From daily MODIS cloud mask products between 2003 and 2012 the low cloud class was extracted and mean low cloud frequency was calculated for Taiwan. This low cloud frequency map was blended with an existing plot-based vegetation classification for Taiwan to analyze the relationship between low cloud frequency and TMCF occurrence. Receiver operating characteristics curves and the area under the ROC curve (AUC) were used to analyze if a relationship exists. No relationship was found for all four TMCF types taken together (AUC = 0.61) and for the dominant TMCF type, Quercus montane evergreen broad-leaved cloud forest (AUC = 0.5). Strong relationships were found for the two spatially-restricted TMCF types, Fagus montane deciduous broad-leaved cloud forest (AUC = 0.91) and Pasania-Elaeocarpus montane evergreen broad-leaved forest (AUC = 0.84), as well as for the second dominant type Chamaecyparis montane mixed cloud forest (AUC = 0.74). The results show that low cloud frequency thresholds might be associated with specific cloud forest types in Taiwan. Further studies should incorporate information about cloud base height, cloud

density, and cloud immersion time as well as satellite-based cloud frequency information with a higher temporal resolution. Combination with satellite-based land cover classifications for Taiwan would allow quasi-continuous observation of TMCF changes. Such knowledge would be the precondition for effective protective actions concerning this exceptional but threatened ecosystem.

Keywords: Taiwan; tropical montane cloud forest; satellite; MODIS; vegetation survey

1. Introduction

Tropical montane cloud forests (TMCF) represent a rare and exceptional ecosystem of the humid tropics. They are generally characterized by the frequent or permanent occurrence of low clouds [1] but their form and appearance varies globally and depends upon latitude, altitude, topography, distance to the ocean, wind direction, and rainfall patterns [2,3]. In addition to their important role regarding regional ecosystem water services (e.g., [4]), they are biodiversity hotspots and known for their exceptionally high endemism (e.g., [5]). Unfortunately, their water resources and their specific biodiversity are globally threatened by climate change [6,7] and land use change [8,9].

The urgent protection of cloud forest sites requires a comprehensive knowledge about their regional occurrence. However, the precise mapping of TMCFs is challenging because various abiotic and biotic factors determine their location [3]. Although researchers have been active for many years, there are still uncertainties about the large variety of subtropical and tropical cloud forest ecosystems [10]. The range of altitudes at which cloud forests are found is impressive (220–5005 m). The climate of cloud forests is highly variable from forest to forest, with an average rainfall of about 2000 mm per year and an average temperature of 7–17 °C [11].

Maps based on ground-measured floristic or physiognomic characteristics have been used to map TMCF at the spatial scales of a single montane or landscape (e.g., [12]). Other approaches have used elevation as a proxy for the climatic (temperature, rainfall, and fog incidence) and edaphic (soil water status, acidity) conditions that tend to be associated with cloud forests (e.g., [3,13]). TMCF mapping would explicitly account for multiple climatic and physiographic factors, including cloud frequency, wind and rainfall patterns, as well as aspect, latitude, altitude, the size of montanes, their distance from the sea, and local vegetation classification [10]. Li *et al.* [14] investigated nine abiotic factors for cloud forests in Taiwan and stated that temperature and moisture are the dominant factors.

Despite the occurrence of TMCFs in a wide range of climatic and landscape situations [11], the main common climatic attribute for every TMCF is frequent and persistent cloud immersion [6,15,16] and the global, regional, and local factors that influence cloud formation. Temperature and moisture govern cloud condensation, influenced by offshore sea surface temperatures, land–sea interactions involving the size of a montane and its orientation and exposure to the prevailing winds [1,11,17,18]. Cloud forests are uniquely separated from other montane forests only on the basis of the cloud immersion time [19]. High frequency of low level clouds is a key factor affecting TMCF. The clouds strongly influence the radiation budget and the humidity regime of the forest [20–23].

Mulligan and Burk [19] and Mulligan [24] successfully utilized satellite-based cloud frequency data in combination with climate and land cover data to map TMCF distribution as 'forest under frequent and/or persistent exposure to ground-level cloud'. For their TMCF map they found an overestimation of the mapped cloud forest area as well as detection problems in highly-heterogeneous areas. Much of the overestimation and the detection problems were due to the coarse cloud climatology used. They suggest to use the Moderate-Resolution Imaging Spectroradiometer (MODIS) cloud mask with a spatial resolution of 1 km [25–28] instead.

Nair *et al.* [29] used the MODIS cloud product together with reanalysis data to quantify cloud-immersion statistics for tropical montane cloud forests in Northern Costa Rica for March 2003. They used the 11μm channel in conjunction with reanalysis data to estimate cloud-top heights. The cloud optical thickness was used with empirical and adiabatic model approaches to estimate cloud thickness. The cloud-base height was calculated from the cloud-top height and the cloud thickness. This was compared with a digital elevation model (DEM) to determine cloud immersion. Problems occur with the MODIS cloud product which does not always successfully retrieve cloud properties. In addition to missing values, the retrieved values of cloud optical depth may not fall within the range in which cloud-base height can be accurately estimated. For both situations it was not possible to compute cloud immersion. As a consequence, the real cloud immersion frequency was underestimated. Nair *et al.* [29] concluded to use multiple years of data to obtain reliable cloud immersion frequencies. Additionally, the simplified assumptions about the vertical profile of the cloud liquid water content (empirical and adiabatic) can lead to inaccuracies in the estimated cloud thickness [30,31].

With respect to the mapping of TMCF using satellite-based cloud frequencies it has to be stated that there is no universally agreed-upon definition of the frequency, duration or extent to which a tropical forest must be immersed in clouds to be defined as a TMCF. For their quantified cloud-immersion statistics for March 2003 Nair *et al.* [29] did not infer such a frequency threshold. Mulligan and Burk [19] and Mulligan [24] obtained the best fit between actual and modeled cloud forest presence for a cloud frequency threshold of at least 70%. It is recognized that this is a relatively high level of cloud frequency. In this context, the authors refer to the fact that there are no data sets for the absence of cloud forests. Therefore, they rely solely on the validation using presence records. The disadvantage of this approach is that the greater the area a threshold defines as cloud forest, the greater will be its potential hit-rate and thus the better the validation will appear. A more extensive data set with detailed information about the occurrence and absence of TMCF plots could mitigate this problem. This would allow the calculation of the true positive rate (hit-rate) together with the false positive rate. The appropriate cloud frequency threshold could be determined for the optimal combination of a high true positive rate together with a low false positive rate.

Such an extensive ground-based vegetation dataset is available for Taiwan [14]. The plots were sampled between 2003 and 2007 during a vegetation mapping project organized by the Taiwan Forestry Bureau [32]. Using plots sampled during a vegetation mapping project organized by the Taiwan Forestry Bureau between 2003 and 2007 [32] Li *et al.* [14] recognized 21 main forest types. Among them, four forest types were described as montane cloud forest. Additionally, with this extensive ground-based observation dataset no area-wide information on the spatial distribution of TMCF in Taiwan is hitherto available. The limited knowledge and, at the same time the observed loss of TMCF in Taiwan, for

example due to high montane tea plantation [33], call for an overall mapping of this threatened ecosystem in Taiwan to support decision processes for the establishment of protected TMCF areas.

Therefore, the aim of the current study is to use the new available vegetation dataset in combination with a ten year time-series of low cloud frequencies (i.e. frequency of low cloud occurrence) from the MODIS cloud mask product in 1 km resolution to investigate the relationship between the occurrence of TMCF and low cloud frequencies in Taiwan for the first time. Such a relationship would offer the possibility for area-wide cloud forest classification in Taiwan by means of a satellite-based cloud frequency threshold.

2. Material and Methods

2.1. Study Area

Taiwan (21°52'–25°17'N, 119°58'–122°00'E) is located in the subtropics on the eastern margin of the Eurasian Plate and borders the most western extensions of the Pacific Ocean. The island is dominated by the Central montane Range (CMR) which runs from north to south (Figure 1). The CMR covers about two-thirds of the entire area of Taiwan and has an average height of approximately 2000 m, including more than 200 peaks above 3000 m above sea level (a.s.l.). The highest peak in Taiwan is Mt. Yushan with 3952 m a.s.l. [14,34].

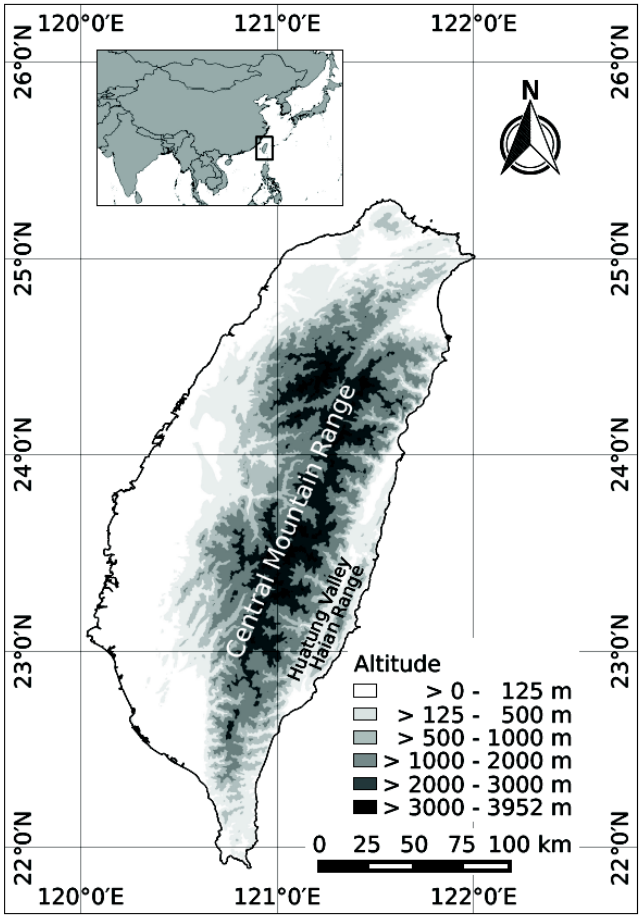

Figure 1. Topography (derived from SRTM DEM, U.S. Geological Survey) and geographical location of Taiwan.

The island's heterogeneous topography influences rainfall patterns, as well as atmospheric circulation, and causes large spatial variations in the regional climate which, on a larger scale, is predominantly affected by the East Asian Monsoon. The northeasterly monsoon hits Taiwan from September to April, whereas the southwesterly monsoon occurs from May to August [35]. The mean annual precipitation of the island varies from 1300 mm y^{-1} in the west and 2500 mm y^{-1} in the east, to more than 4000 mm y^{-1} in some regions of the CMR [36]. The diurnal course of the weather is characterized by daytime upslope-onshore and night-time down-slope-off-shore breeze systems which correspond to the diurnal heating-cooling cycle. Related to the thermal forcing, rainfall rates and cloud coverage reach their maximum in the late afternoon [37].

Almost 60% of Taiwan's area is still covered by forests, out of which 73% are natural forest, 20% plantation and 7% bamboo, data from [38]). Natural forests have been replaced by the increasing expansion of farmland and cities particularly in the coastal lowlands of the island's western part. To date, the pristine TMCF is limited to steep and poorly-accessible areas of the CMR, naturally disturbed by landslides after heavy rainfall events, sometimes related to typhoons [14,39–41].

2.2. Data

2.2.1. MODIS Cloud Mask

For the current study, MODIS (Moderate Resolution Imaging Spectroradiometer) products from 2003 to 2012 were used. The 1 km MODIS Cloud Mask product (MOD35/MYD35) [25–28], including information on cloud occurrence and cloud type, was considered.

The MODIS Cloud Mask [25–28] is available at 250 m and 1 km resolution. For the current study the 1 km cloud mask is considered since it provides information about cloud types. It uses 19 of the existing 36 spectral bands that measure at wavelengths from 400 nm to 14.5 μm and consists overall of 48 bits (6 bytes) per pixel. Every bit represents a flag (yes-no decision) and indicates the results of the tests executed. The MODIS cloud mask and all tests are extensively discussed by Ackerman *et al.* [27]. Cloud masking algorithm uses differences between 11 and 3.9 micron channels to identify low level clouds. Large negative values of this difference in daytime scenes are indicative of the presence of low level clouds. In addition, visible reflectance thresholds of the 0.65 micron channel are also used, which indicate the presence of bright clouds.

The data for the ten years period were downloaded for every day in HDF format from the NASA FTP server (ftp://ladsweb.nascom.nasa.gov/allData/5/). Per day two scenes are available:

- Terra overflight: *ca*. 2:00 am–3:30 am UTC, 10:00 am–11:30 am local time
- Aqua overflight: *ca*. 4:30 am–6:00 am UTC, 12:30 pm–2:00 pm local time

The metadata of the downloaded cloud mask products provide additional information about the exact geographical coordinates. The included latitude and longitude coordinates for each pixel were used to project the data to UTM-51N by nearest neighbor resampling.

2.2.2. Vegetation Dataset

The vegetation dataset used in this study is a subset of the National Vegetation Database of Taiwan consisting of vegetation plots from different altitudes and habitats. The plots were sampled between 2003 and 2007 during a vegetation mapping project organized by the Taiwan Forestry Bureau [32]. Based on species composition Li *et al.* [14] recognized 21 main forest types. Among them, four forest types (Table 1) were described as montane cloud forest whose geographical distribution were supposed to be correlated with cloud frequency (Figure 2).

Table 1. Number of considered plots for 19 forest types (4 TMCF and 15 non-TMCF) in Taiwan coded and classified by Li *et al.* [14].

Code	Forest Type	No. of plots
	Tropical Montane Cloud Forest	
C2A03	Chamaecyparis montane mixed cloud forest	383
C2A04	Fagus montane deciduous broad-leaved cloud forest	30
C2A05	Quercus montane mixed cloud forest	565
C3A09	Pasania–Elaeocarpus montane evergreen broad-leaved cloud forest	39
	TMCF plots	1017
	Non-Tropical Montane Cloud Forest	
C2A06	Machilus–Castanopsis sub-montane evergreen broad-leaved forest	199
C2A07	Phoebe–Machilus sub-montane evergreen broad-leaved forest	191
C2A08	Ficus–Machilus foothill evergreen broad-leaved forest	56
C3A10	Drypetes–Helicia sub-montane evergreen broad-leaved forest	134
C3A11	Dysoxylum–Machilus foothill evergreen broad-leaved forest	6
	Non-TMCF plots	586
	All considered plots	1603

The montane cloud zone is characterized by clouds frequently descending to the ground. Dominant tree species are adapted to frequent fogs by spherical crowns, which are efficient in making the best use of diffuse light [42].The sub-montane zone is dominated by umbrella-shaped tree crowns, which are more efficient for the interception of direct sunlight. Due to strong human impact, most of the old-growth forests in the foothill zone are restricted to stony slopes and shaded valleys, which cannot be used for agriculture. The crown shape is round because of the shaded habitat.

Chamaecyparis montane mixed cloud forests (C2A03) are located at higher altitudes of the subtropical montane cloud zone (mean altitude: 2200 m) on middle slopes, upper slopes, and ridges. The Kira's warmth index (WI; [43]), defined as the annual sum of positive temperature differences between monthly means and 5 °C, varies between 100 and 150 °C. The mean precipitation amount calculated from the WorldClim global climate dataset [44] for the plots considered by Li *et al.* [14] is about 3300 mm from which a great part falls in the winter season (December to February) [35]. Fagus montane deciduous broad-leaved cloud forests (C2A04) are restricted to ridges in the northern part of Taiwan (mean altitude: 1900 m, Kira's warmth index: 130–160 °C). The mean precipitation amount for these plots is about 2700 mm. Most of the precipitation falls in the winter season [35]. In contrast to C2A03

forests, Quercus montane evergreen broad-leaved cloud forests (C2A05) occur at lower altitudes of the montane cloud zone (mean altitude: 1800 m, Kira's warmth index: 90–180 °C). At the same altitude, C2A05 forests can be found on more shaded and steeper slopes with shallower, rockier soils compared to C2A03 forests. The mean precipitation amount calculated for the C2A05 plots is about 3000 mm. The main part of the precipitation falls during the spring transition (March and April) and during the summer season (mid-July to late August) [35]. The occurrence of Pasania–Elaeocarpus montane evergreen broad-leaved cloud forests (C3A09) is restricted to the southernmost peak of Taiwan with an altitude above 2000 m (mean altitude: 1500 m, Kira's warmth index: 175–190 °C). On average the C3A09 plots receive about 4800 mm precipitation per year, from which the main part falls during the spring transition and the summer monsoon season [35].

To analyze the relationship between montane cloud forest types and cloud frequency the four montane cloud forest types were considered as TMCF. The remaining subtropical and tropical montane zonal forest types were considered as non-TMCF (Table 1).

Figure 2 shows the spatial distribution of the 1017 plots across the TMCF and the non-TMCF plots. For a detailed description of the respective forest types and their dominant species refer to Li *et al.* [14].

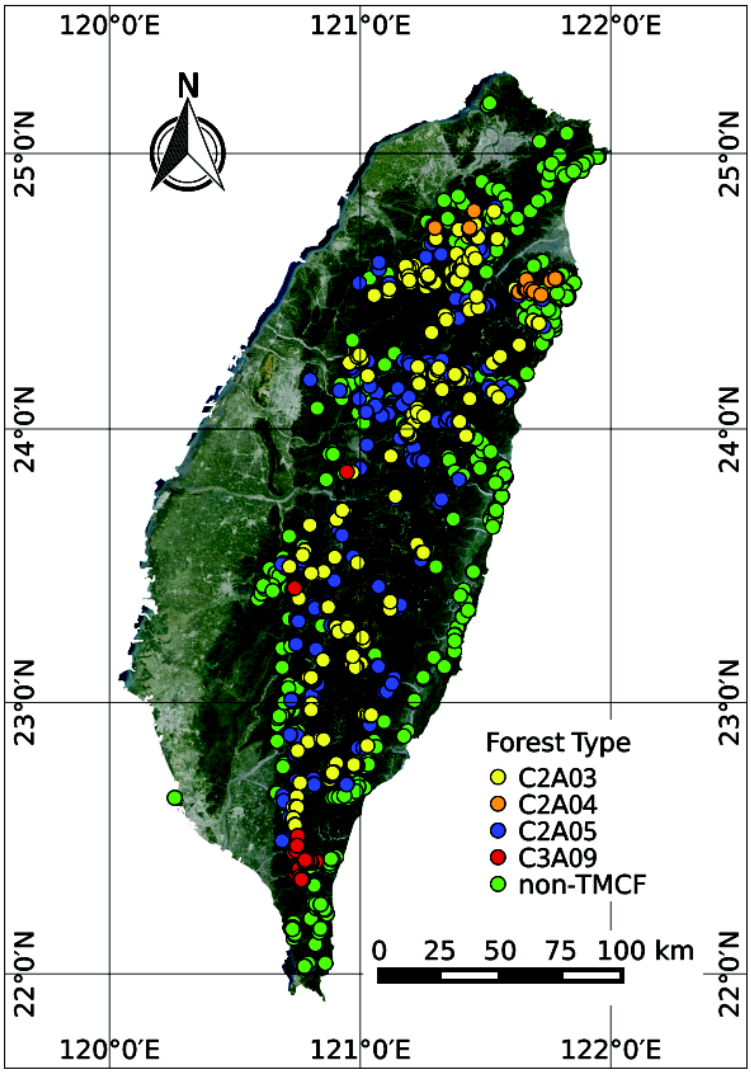

Figure 2. Spatial distribution of all 1603 TMCF and non-TMCF plots in Taiwan considered in this study. A Landsat 8 image is underlying.

2.3. Methods

2.3.1. Calculation of the Low Cloud Frequency Map

For the analysis of the relationship between low cloud frequency and TMCF occurrence, 11 and 3.9 micron difference test and visible reflectance test (see Section 2.2.1) results in the MODIS cloud mask data set are used to detect the presence of low level clouds. A binary cloud mask is then generated indicating the presence or absence of low level clouds. The elevation of the terrain was neither explicitly taken into account nor was there any terrain correction applied. Subsequently, the average low cloud frequency between 2003 and 2012 was calculated [27].

2.3.2. Investigating the Relationship between Cloud Forest Occurrence and Low Cloud Frequency

To investigate the relationship between the occurrence of TMCF and low cloud frequency in Taiwan, the calculated average low cloud frequency was extracted for each location of the vegetation plots. Receiver Operating Characteristics (ROC) curves and the Area Under ROC Curve (AUC) [45,46] were used to analyze if a relationship exists.

Receiver Operating Characteristics (ROC) curves were identified as suitable for the analysis of the relationship between cloud frequencies and cloud forest occurrence. ROC curves indicate the performance of a binary classifier as its threshold is varied between the minimum and the maximum values. The curve is created by plotting the true positive rate against the false positive rate for each threshold value. The true positive rate defines the proportion of positives that are correctly identified as such (e.g., the percentage of TMCF plots that are correctly identified as TMCF). It is calculated with:

$$truepositiverate = \frac{truepositive}{truepositive + falsenegative} \quad (1)$$

with true positive: positives correctly identified as such, false negative: positives incorrectly identified as negative.

The false positive rate defines the proportion of positives that are incorrectly identified as such (e.g., the percentage of non-TMCF plots that are incorrectly identified as TMCF). The false positive rate is calculated with:

$$falsepositiverate = \frac{falsepositive}{falsepositive + truenegative} \quad (2)$$

with false positive: negatives incorrectly identified as positives, true negative: negatives correctly identified as such.

Table 2. Idealized dataset used for the construction of the ROC curve and the calculation of the AUC in Figure 3.

Cloud Frequency	**1**	**0.9**	**0.8**	**0.7**	**0.6**	**0.5**	**0.4**	**0.3**	**0.2**	**0.1**	**0**
TMCF	1	1	1	1	0	0	0	0	0	0	0
Non-TMCF	0	0	0	0	1	1	1	1	1	1	1

Note: 1 = respective forest type present; 0 = respective forest type not present.

The area under the ROC curve (AUC) provides a single measure of overall the accuracy of a binary classifier that is not dependent upon a particular threshold. By summarizing the overall performance over all possible thresholds, it is therefore possible to analyze the relationship between cloud forest occurrence and cloud frequency. The AUC values range from 0 to 1 and specify the probability with which TMCF and non-TMCF plots can be separated by means of the cloud frequency. A value of 1 would indicate a perfect classification. A value of 0.5 corresponds to a random classification performance.

Figure 3 shows an example of a ROC curve and the calculated AUC value for the idealized dataset in Table 2. A perfect classification would yield a point in the upper left corner coordinate (false positive rate: 0, true positive rate: 1) of the ROC space, representing no false negatives and no false positives. The (0,1) point is also called a perfect classification. This would result in an AUC value of 1. The diagonal line (line of no-discrimination) divides the ROC into good classification results above the diagonal represent (better than random) and poor classification results below the line poor results (worse than random). A completely random guess would give a point along a diagonal line from the left bottom to the top right corner. The corresponding AUC value would be 0.5. In our example we iterated the cloud frequency threshold between 0 and 1. The resulting combinations of true positive rate and false positive rate for each threshold value are indicated by the colored line which illustrates the relationship between low cloud frequency and the occurrence of TMCF. In this case the ideal cloud frequency threshold would be 0.7 resulting in a perfect TMCF classification with an AUC value of 1.

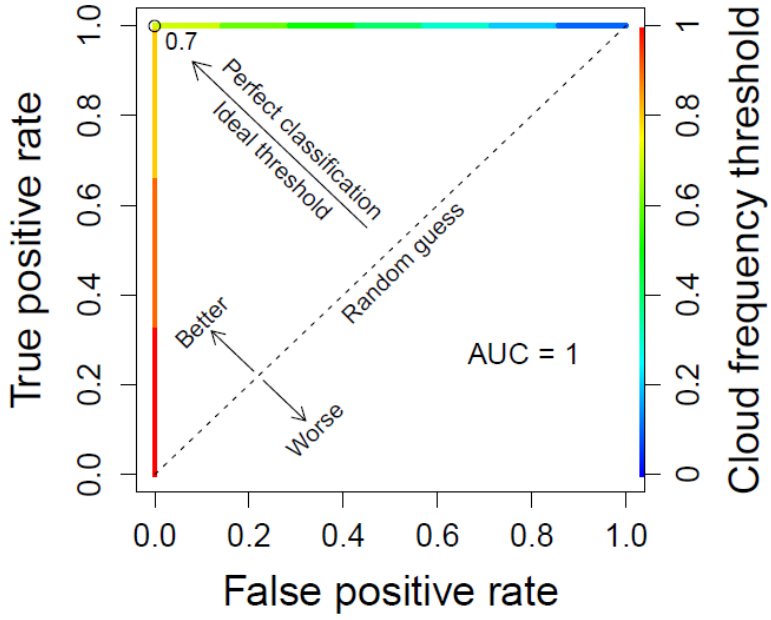

Figure 3. Idealized ROC curve which theoretically reveals a strong relationship between the frequency of low clouds.

To create the ROC curve and calculate the AUC in the current study, the extracted cloud frequency for every vegetation plot served as a reference. The cloud frequency threshold to classify TMCF was iterated between the maximum cloud frequency and the minimum cloud frequency. All TMCF plots with an extracted cloud frequency above the respective cloud frequency threshold were indicated as true positive, whereas all TMCF plots below the respective cloud frequency threshold were indicated as false negative. From the amount of the true positive and false negative plots the true positive rate was

calculated with Equation (1). All non-TMCF plots with an extracted cloud frequency above the respective cloud frequency threshold were indicated as false positive, whereas all non-TMCF plots below the respective cloud frequency threshold were indicated as true negative. From the amount of the false positive and true negative plots the false positive rate was calculated with Equation (2). For each cloud frequency threshold between the maximum and the minimum cloud frequency we thus obtained a true positive rate and a false positive rate that were used to create the ROC curve and calculate the AUC.

3. Results

3.1. Distribution and Frequency of Low Clouds

The calculated frequency and distribution of low clouds over Taiwan from 2003 to 2012 is displayed in Figure 4. The occurrence of low clouds is related to the island's topography (*cf*. Figure 1). Peaks, ridges, and plateaus of the CMR above 2000 m altitude show the highest frequencies of low cloud occurrences (20% to 36%). The northeastern and southern foothills of the CMR, as well as the north-south elongated and up to 1600 m a.s.l. high Haian Range—located at the southeastern coast (*cf*. Figure 1)—also reveal similar values. On the contrary, the western plain and the dominant Huatung Valley in the east (*cf*. Figure 1) are less often covered by low clouds (<20%). Moreover, an evident difference is noticeable between east- and west-facing valleys. The frequency of low cloud occurrences is low in the eastern valleys but reaches an absolute minimum in the center of west or southwest exposed valleys.

3.2. Relationship between Cloud Forest Occurrence and Low Cloud Frequency

Figure 5 shows the calculated ROC curves and AUC values. No relationship between low cloud frequency and the occurrence of all four TMCF types taken together can be stated. The AUC value of 0.61 indicates that high frequencies were only slightly more often observed for cloud forest plots than for the other forest plots.

In a next step ROC curves were calculated separately for the four cloud forest types. The restricted sites of Fagus montane deciduous broad-leaved cloud forests (C2A04; Figure 5b) in the northeastern part (AUC = 0.91) and of Pasania–Elaeocarpus montane evergreen broad-leaved cloud forests (C3A09; Figure 5d) in the tropical part of Taiwan (AUC = 0.84) (*cf*. Figure 1) could be related to the frequency of low clouds. The relationship between the Chamaecyparis montane mixed cloud forest (C2A03; Figure 5a) and low clouds was somewhat weaker (AUC = 0.74) but still notable. However, the Quercus montane evergreen broad-leaved cloud forest (C2A05; Figure 5c) which is scattered over the entire CMR does not reveal any relation to high frequencies of low cloud occurrences (AUC = 0.5).

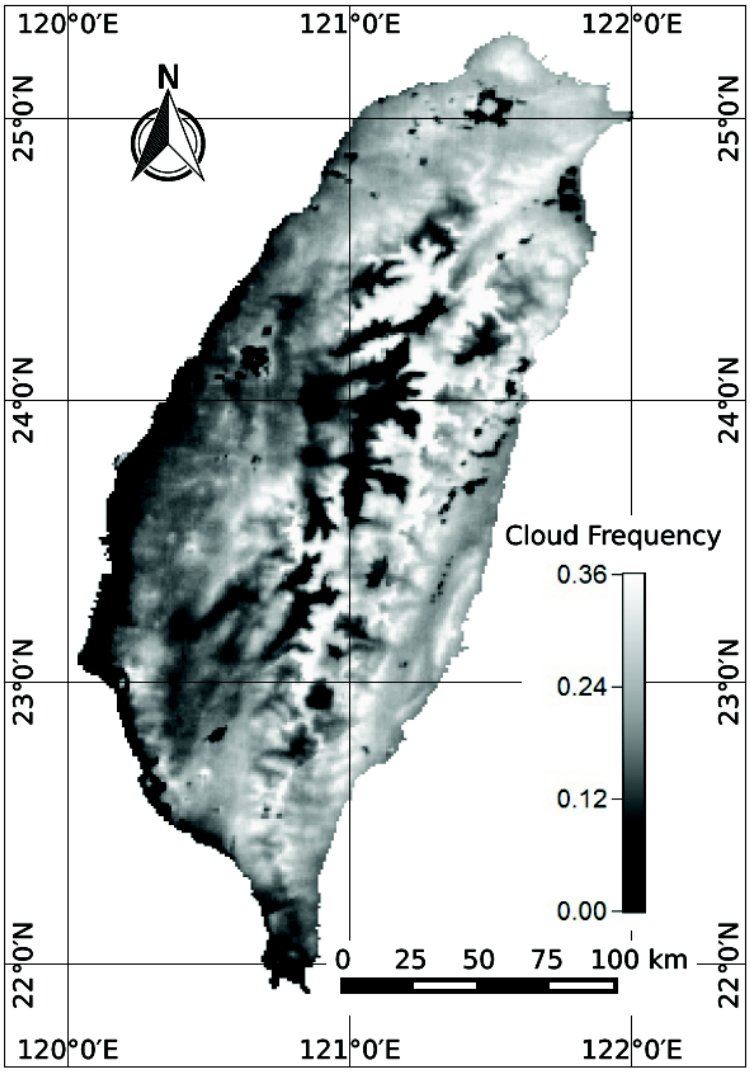

Figure 4. Average daytime (late morning to early afternoon) low cloud frequency over Taiwan based on Terra and Aqua MODIS data from 2003 to 2012.

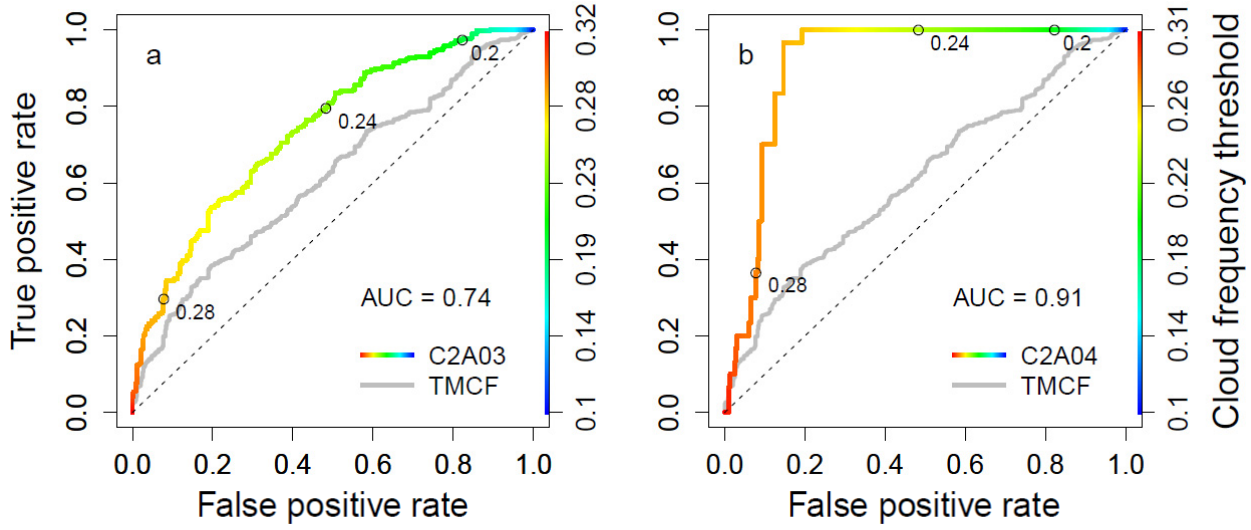

Figure 5. *Cont.*

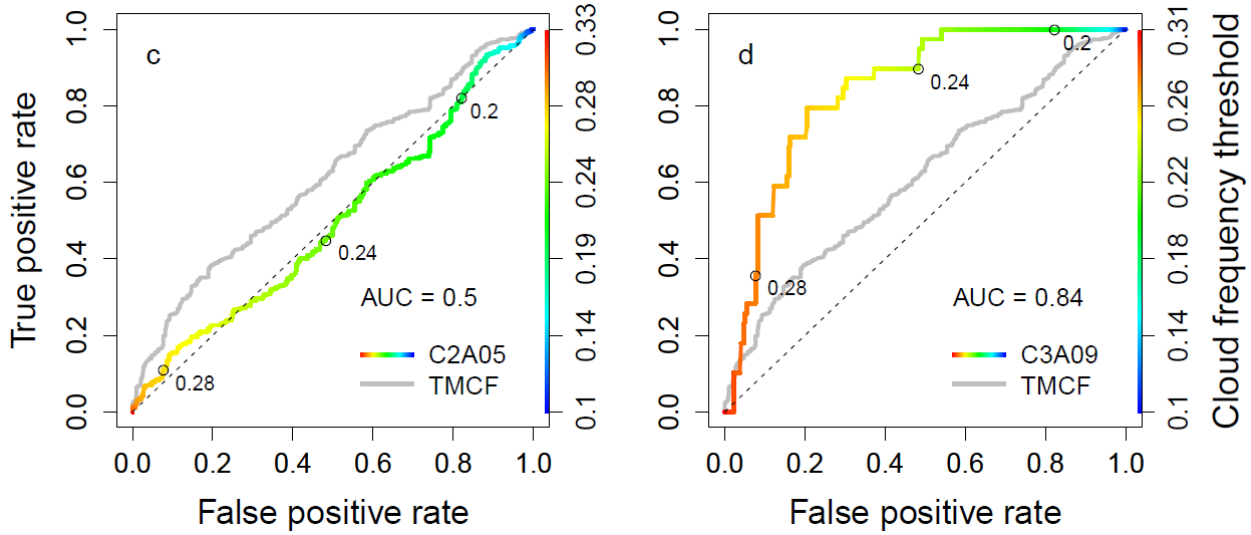

Figure 5. ROC curves showing the relationship between the four TMCF types C2A03 (**a**), C2A04 (**b**), C2A05 (**c**), and C3A09 (**d**) and daytime low cloud frequency in Taiwan. The additional grey ROC curve (AUC = 0.61) indicates the relationship between all TMCF types and low cloud frequency. The color bar indicates the respective cloud frequency threshold used for ROC calculation (blue = lowest frequency, red = highest frequency).

4. Discussion

The calculated area under curve values indicate strong relationships between low clouds and the subtropical Fagus montane deciduous broad-leaved cloud forest (C2A04, AUC = 0.91) and the tropical Pasania-Elaeocarpus montane evergreen broad-leaved forest (C3A09, AUC = 0.84). However, it should be considered that the small population size and the limited spatial distribution may have influenced the results.

The spatial distribution and clustering of the specific TMCF types in Taiwan is probably the result of the seasonal weather cycle and the resulting spatial distribution of high frequency of low cloud cover and high precipitation amounts.

Fagus montane deciduous broad-leaved cloud forest (C2A04) occurs only on ridges in the northern part of Taiwan (mean altitude 1900 m). Together with the southwest coast these areas receive the highest precipitation rates in Taiwan [36]. The high degree of topographic exposure to cloud and rainfall bearing winds probably determines the local conditions for the development of Fagus cloud forest in this region and might be the reason for the strong relationship between low cloud frequency and the occurrence of Fagus montane cloud forest. The high frequencies of low clouds for the northeastern foothills of the CMR (Figure 4) are probably linked to the main rainfall period during winter. The stable or slightly unstable stratification and low air moisture content lead to extended stratiform cloud cover and precipitation with high rainfall rates on the wind-exposed slopes at the north and northeast coast [47,48]. A second but smaller cloud cover and precipitation maximum occurs during autumn (September to November) mainly due to "late" typhoons [35]. During the summer season the Fagus cloud forests receive only medium precipitation amounts.

Pasania–Elaeocarpus montane evergreen broad-leaved cloud forest (C3A09; mean altitude 1500 m) occurs to the south of Yi-Ding Shan, the southernmost peak with an altitude above 2000 m. Some isolated plots are found on west-facing slopes in the middle part of the CMR. Together with the north

and northeast coast these areas receive the highest rainfall rates in Taiwan. All C3A09 sites are found on upper slopes and ridges characterized by strong winds due to a lack of topographic shading. As before, for the Fagus cloud forest, it can be assumed that the high topographical exposure of the sites and the corresponding high water input by clouds and rain determines the local conditions for the development of Pasania–Elaeocarpus cloud forest in this region which could explain the strong relationship between its occurrence and low cloud frequency. The high frequencies of low clouds for the southern foothills of the CMR (Figure 4) are in accordance with the precipitation dynamic in this area. The main rainfall seasons are the spring transition (March and April) with convective clouds and precipitation mainly at the southwest-facing slopes of the CMR [35,48], the summer season with tropical storms [49] and the southwesterly monsoon flow [51] with cloud and rainfall maxima at the west and southwest coast.

In contrast to C2A04 and C3A09 Chamaecyparis montane mixed cloud forests (C2A03) and Quercus montane evergreen broad-leaved cloud forests (C2A05) are distributed over the entire CMR and represent the two most common forest types in Taiwan. For C2A03 we could find a strong relationship between its occurrence and low cloud frequency (AUC = 0.74). Chamaecyparis montane mixed cloud forest is located at higher altitudes of the montane cloud zone with a local concentration in the southern and northern part of the western slopes of the CMR. With a mean altitude of 2200 m most of the plots are situated above the cloud condensation level most of the time. As can be seen in the cloud frequency map (Figure 4) peaks, ridges and plateaus of the CMR above 2000 m altitude show the highest frequencies of low cloud occurrences (20% to 36%). This would explain the good relationship between low cloud frequency and the occurrence of Chamaecyparis montane cloud forest. Apart from the high water input due to cloud immersion Chamaecyparis cloud forests receive a considerable amount of rainfall. The northwesterly wind-exposed slopes receive most of the precipitation during the winter monsoon season (December to February) [49,50]. The southwestern parts receive their rainfall maximum during the mei-yu (mid-May to mid-June) [50,51] and summer monsoon (mid-July to late August) season [53,54].

As a consequence of the results it would be possible to map the spatial distribution of C2A03, C2A04, and C3A09 in Taiwan using a threshold for low cloud frequency in combination with a satellite-based land cover classification. Inspecting Figure 5 it might be possible to associate cloud frequency with specific cloud forest types. An optimal result with a high true positive rate and a low false positive rate would be obtained for a cloud frequency threshold greater than 24% for C2A03. For C3A09 the appropriate cloud frequency threshold should be greater than 26% and for C2A04 it should lie above 27%.

For Quercus montane evergreen broad-leaved cloud forest (C2A05) there is no relationship with low cloud frequency (AUC = 0.5). Because of the dominance of C2A05 forests (565 plots) the weak relationship between the TMCF plots as a whole and low cloud frequency (AUC = 0.61) is mainly ascribed to the disproportional statistical influence of C2A05 forests. The missing relationship between low cloud frequency and the occurrence of C2A05 hampers its mapping based on a cloud frequency threshold. Quercus cloud forests are either less dependent on the frequent occurrence of low clouds or other unavailable environmental factors are more important.

The more than 560 tropical sites with confirmed cloud forest presence [55] represent a wide range of climatic (temperature, wind, rainfall) and landscape conditions (altitude, montane size, exposure, and distance to sea). Jarvis and Mulligan [11] analyzed the predominant climatic conditions for areas of known cloud forests in the World Conservation Monitoring Centre (WCMC) database of protected

areas [55]. In general, topographical exposure was the most significant parameter explaining the geographical differences between cloud forests and montane forests, followed by distance to coast, montane range size, and altitude [11]. Despite the occurrence of TMCFs in a wide range of climatic and landscape conditions [11], the main common climatic attribute for every TMCF is frequent and persistent cloud immersion [6,15,16] and the factors that influence cloud formation. Temperature, moisture, and nature of the cloud condensation nuclei govern cloud condensation. Other factors like offshore sea surface temperatures, land–sea interactions involving the coastal plain, the size of a montan,e and its orientation and exposure to the prevailing winds provide atmospheric forcing that leads to upward motion which leads to cloud formation [1,11,17,18]. As a consequence, high cloud frequency is assumed to be one of the most significant climatic variables for cloud forests and the reason why altitude, temperature, and distance to coast are important to cloud forest distribution.

For Taiwan, Li *et al.* [14] analyzed nine abiotic factors (altitude, slope, aspect, topography, soil rockiness, whole-light space [56], Kira's warmth index [43,57], annual precipitation, and winter precipitation [44]) with respect to the occurrence of cloud forests. They identified temperature and moisture as the most important factors. The diversity of forest vegetation in Taiwan is strongly structured by the temperature and moisture gradient. In almost all the other environmental parameters Quercus cloud forests (C2A05) show a greater variance due to their scattered distribution.

Quercus forest occurs at lower altitudes of the montane cloud zone (mean altitude 1800 m), along the western slopes of the CMR, and in east-facing valleys of the CMR. The western slopes of the CMR are characterized by high cloud coverage and high precipitation rates during the spring transition, the mei-yu season and during the summer monsoon with an absolute minimum during the winter months. Kao *et al*. [36] identified a rainfall maximum with high intensities in the middle to the northern region of the western slopes of the CMR. In this area we can also find a relative concentration of C2A05. In comparison, the eastern areas receive much less rainfall with the highest amount during the winter monsoon and only medium rainfall rates during the summer months [35,47]. In addition to the lower rainfall receipt for this area [36], lower intensities together with a higher number of raining days were found compared to the western slopes. The diurnal cycle might explain the high number of raining days as well as the lower intensities. The diurnal weather at the east coast is characterized by daytime upslope-onshore and nighttime down-slope-off-shore flow and corresponds with the diurnal heating cycle due to the combined effects of orographic lifting and solar heating and the corresponding land-sea breeze system [37]. Rainfall rates and cloud coverage are noticed to reach their maximum in the late afternoon. Concerning a potential relationship between cloud frequency and C2A05 occurrence the cloud and rainfall maximum in the late afternoon at the east-facing slopes was probably not detected by the MODIS midday overpass. This could explain the missing relationship for the east coast in contrast to the west coast were we could expect a strong relationship comparable to C2A03. The spatial occurrence of C2A05 on the west coast is probably mainly due to the high precipitation rates in the respective areas, while C2A03 forests are located at higher altitudes of the montane cloud zone and benefit from this additional water input.

A higher temporal resolution provided by geostationary (GEO) satellite systems (e.g., Himawari-8) might be able to detect the described afternoon cloud and rainfall maximum. To obtain a comparable 1 km resolution an appropriate pansharpen algorithm (e.g., [58]) could be applied. Another aspect that could be important beside the cloud frequency is the cloud density together with the fog duration.

Mildenberger *et al.* [23] state that high frequency and high density of fog strongly influences the radiation budget and, obviously, the humidity regime at the altitude ranges where cloud montane forests occur. GEO systems with their higher temporal resolution could help to analyze the cloud immersion time in more detail. With respect to the cloud density, analyzing the cloud optical thickness from the MODIS cloud product might give useful insights. Unless we will have further information about the density of cloud events and the length of its lasting time, Quercus montane cloud evergreen broad-leaved forests (C2A05) cannot be well mapped only by cloud frequency.

The MODIS cloud mask is suitable for the generation of high resolution cloud frequency maps as presented in this work. Nonetheless, it is necessary to be aware of the limited validity and accuracy of the applied cloud masks and the final low cloud frequency map. Low clouds covered by overlying high clouds are not represented in the cloud frequency map. Thus, the calculated low cloud frequency is expected to be slightly lower than in reality. However, due to the long-time observation period, the reoccurring non-detection of obstructed low clouds is supposed to not significantly influence the distribution of the calculated low cloud frequencies.

One uncertainty in the presented approach related to the detection of TMCF is the unknown cloud base height of the identified low clouds. Therefore, a differentiation between cloud immersion and those low clouds that do not directly interact with the biosphere was not possible. For the occurrence and mapping of TMCF it is essential to detect cloud immersion of the terrain. The approach by Nair *et al.* [29] offers the possibility to determine cloud base height. However, due to the inherent uncertainties concerning the determination of the cloud top height and cloud thickness together with problems concerning the MODIS cloud product this approach does not seem suitable for TMCF mapping in Taiwan at the moment. In this context it has to be stated that we are currently working on a 250 m ground-fog detection scheme based on MODIS data, which would hopefully overcome the existing problems.

5. Conclusions

The aim of the current study was to investigate the relationship between the occurrence of Tropical Montane Cloud Forest (TMCF) and low cloud frequency in Taiwan for the first time. For this purpose, we have taken a hydrological definition of cloud forest as forest under frequent and or persistent exposure to low level clouds. We have used new datasets that have not been explored in Taiwan previously to derive a low cloud frequency map and to analyze the relationship between the calculated low cloud frequency and the occurrence of TMCF based on a new extensive observation dataset of cloud and non-cloud forest classification in Taiwan. To investigate the relationship between the occurrence of TMCF and low cloud frequency, the satellite-based low cloud frequency was compared to ground-based vegetation plots. Receiver Operating Characteristics curves and the Area Under ROC Curve (AUC) were used. For the most abundant TMCF type Quercus montane evergreen broad-leaved cloud forest we could not find a relationship (AUC = 0.5). For the remaining three TMCF types we found clear relationships. Strong relationships were identified for the spatially-restricted sites of Fagus montane deciduous broad-leaved cloud forests (AUC = 0.91) and of Pasania–Elaeocarpus montane evergreen broad-leaved cloud forests (AUC = 0.84). The relationship between the Chamaecyparis montane mixed cloud forest and low clouds was somewhat weaker (AUC = 0.74). The results show that low cloud frequency thresholds might be associated with specific cloud forest types in Taiwan. TMCF classification with high resolution

remote sensing data is important because a comprehensive knowledge about its exact distribution could contribute to the conservation and investigation of this rare and fragile ecosystem. New satellite-based cloud frequency products with a higher temporal resolution could improve the accuracy of the derived cloud frequency threshold and may improve the relationship between the occurrence of most abundant Quercus cloud forest and low cloud frequency. The same holds true for the explicit consideration of the cloud base height to determine cloud contact with the surface and the additional incorporation of cloud density together with cloud immersion time.

Acknowledgments

This research was funded through a grant (TH1531/2-1) from the German Research Council (DFG) in cooperation with the Taiwanese National Science Council (NSC).

Author Contributions

B.T, A.G, and M.S. conceived and designed the experiments; B.T, A.G, M.S., and J.B. analysed the data; C.-F.L. and S.-C.C. contributed materials; B.T. and A.G. wrote the paper with contributions from all coauthors.

Conflicts of Interest

The authors declare no conflict of interest.

References and Notes

1. Hamilton, L.S. Mountain cloud forest conservation and research: A synopsis. *Mount. Res. Dev.* **1995**, *15*, 259–266.
2. Bruijnzeel, L.A.; Hamilton, L.S. *Decision Time for Cloud Forest*; IHP Humid Tropics Programme Series No. 13; IHP, UNESCO: Paris, France, 2000.
3. Bubb, P.; May, I.; Miles, L.; Sayer, J. *Cloud Forest Agenda*; UNEP World Conservation Monitoring Centre: Cambridge, UK, 2004.
4. Postel, S.L.; Thompson, B.H., Jr. Watershed protection: Capturing the benefits of nature's water supply services. *Natural Resources Forum* **2005**, *29*, 98–108.
5. Hsieh, C.F. Composition, endemism and phytogeographical affinities of the Taiwan flora. *Flora Taiwan* **2003**, *6*, 1–14.
6. Foster, P. The potential negative impacts of global climate change on tropical montane cloud forests. *Earth-Science Rev.* **2001**, *55*, 73–106.
7. Nadkarni, N.M.; Solano, R. Potential effects of climate change on canopy communities in a tropical cloud forest: An experimental approach. *Oecologia* **2002**, *131*, 580–586.
8. Ray, D.K.; Nair, U.S.; Lawton, R.O.; Welch, R.M.; Pielke, R.A. Impact of land use on Costa Rican tropical montane cloud forests: Sensitivity of orographic cloud formation to deforestation in the plains. *J. Geophys. Res.: Atmos.* **2006**, *111*, doi:10.1029/2005JD006096.

9. Martínez, M.L.; Pérez-Maqueo, O.; Vázquez, G.; Castillo-Campos, G.; García-Franco, J.; Mehltreter, K.; Landgrave, R. Effects of land use change on biodiversity and ecosystem services in tropical montane cloud forests of Mexico. *Forest Ecol. Manage.* **2009**, *258*, 1856–1863.
10. Scatena, F.N.; Bruijnzeel, L.A.; Bubb, P.; Das, S. Setting the stage. In *Tropical Montane Cloud Forests: Science for Conservation and Management*; Bruijnzeel, L.A., Scatena, F.N., Hamilton, L.S., Eds.; Cambridge University Press: Cambridge, UK, 2010; pp. 3–13.
11. Jarvis, A.; Mulligan, M. The climate of cloud forests. *Hydrol. Process*. **2011**, *25*, 327–343.
12. Frahm, J.P.; Gradstein, S.R. An altitudinal zonation of tropical rain forests using byrophytes. *J. Biogeogr*. **1991**, *18*, 669–678.
13. Campanella, R. The role of GIS in evaluating contour-based limits of cloud forest reserves in Honduras. In *Tropical Montane Cloud Forests*; Hamilton, L.S., Juvik, J.O., Scatena, F.N., Eds.; Springer: New York, NY, USA, 1995; pp. 116–124.
14. Li, C.F.; Chytrý, M.; Zelený, D.; Chen, M.Y.; Chen, T.Y.; Chiou, C.R.; Hsia, Y.-J.; Liu, H.-Y.; Yang, S.-Z.; Yeh, C.-L.; *et al*. Classification of Taiwan forest vegetation. *Appl. Veg. Sci.* **2013**, *16*, 698–719.
15. Scholl, M.; Eugster, W.; Burkard, R. Understanding the role of fog in forest hydrology: stable isotopes as tools for determining input and partitioning of cloud water in montane forests. *Hydrol. Process.* **2011**, *25*, 353–366.
16. Bruijnzeel, L.A.; Mulligan, M.; Scatena, F.N. Hydrometeorology of tropical montane cloud forests: emerging patterns. *Hydrol. Process.* **2011**, *25*, 465–498.
17. Grubb, P.J.; Lloyd, J.R.; Pennington, T.D.; Whitmore, T.C. A comparison of montane and lowland rain forest in Ecuador I. The forest structure, physiognomy, and floristics. *J. Ecol*. **1963**, *51*, 567–601.
18. Stadtmüller, T. *Cloud Forests in the Humid Tropics: A Bibliographic Review*; United Nations University Press: Tokyo, Japan, 1987.
19. Mulligan, M.; Burke, S.M. *DFID FRP Project ZF0216 Global Cloud Forests and Environmental Change in a Hydrological Context*; Final Report; DFID: London, UK, 2005.
20. Elias, V.; Tesar, M.; Buchtele, J. Occult precipitation: sampling, chemical analysis and process modelling in the Sumava Mts., (Czech Republic) and in the Taunus Mts. (Germany). *J. Hydrol*. **1995**, *166*, 409–420.
21. Dawson, T.E. Fog in the California redwood forest: Ecosystem inputs and use by plants. *Oecologia* **1998**, *117*, 476–485.
22. Weathers, K.C.; Lovett, G.M.; Likens, G.E.; Caraco, N.F. Cloudwater inputs of nitrogen to forest ecosystems in southern Chile: Forms, fluxes, and sources. *Ecosystems* **2000**, *3*, 590–595.
23. Mildenberger, K.; Beiderwieden, E.; Hsia, Y. J.; Klemm, O. CO2 and water vapor fluxes above a subtropical mountain cloud forest—The effect of light conditions and fog. *Agr. Forest Meteorol.* **2009**, *149*, 1730–1736.
24. Mulligan, M. Modeling the tropics-wide extent and distribution of cloud forest and cloud forest loss, with implications for conservation priority. In *Tropical Montane Cloud Forests: Science for Conservation and Management*; Bruijnzeel, L.A., Scatena, F.N., Hamilton, L.S., Eds.; Cambridge University Press: Cambridge, UK, 2010; pp. 14–38.
25. Ackerman, S.A.; Strabala, K.I.; Menzel, W.P.; Frey, R.A.; Moeller, C.C.; Gumley, L.E. Discriminating clear sky from clouds with MODIS. *J. Geophys. Res.: Atmos.* **1998**, *103*, 32141–32157.

26. Ackerman, S.A.; Holz, R.E.; Frey, R.; Eloranta, E.W.; Maddux, B.C.; McGill, M. Cloud detection with MODIS. Part II: validation. *J. Atmos. Ocean. Tech.* **2008**, *25*, 1073–1086.
27. Ackerman, S.; Strabala, K.; Menzel, P.; Frey, R.; Moeller, C.; Gumley, L. *Discriminating Clear-Sky from Cloud with MODIS Algorithm Theoretical Basis Document (MOD35)*; MODIS Cloud Mask Team, Cooperative Institute for Meteorological Satellite Studies, University of Wisconsin: Madison, WI, USA, 2010.
28. Frey, R.A.; Ackerman, S.A.; Liu, Y.; Strabala, K.I.; Zhang, H.; Key, J.R.; Wang, X. Cloud detection with MODIS. Part I: Improvements in the MODIS cloud mask for collection 5. *J. Atmos. Ocean. Tech.* **2008**, *25*, 1057–1072.
29. Nair, U.S.; Asefi, S.; Welch, R.M.; Ray, D.K.; Lawton, R.O.; Manoharan, V.S.; Mulligan, M.; Sever, T.L.; Irwin, D.; Pounds, J.A. Biogeography of tropical montane cloud forests. Part II: Mapping of orographic cloud immersion. *J. Appl. Meteorol. Climatol.* **2008**, *47*, 2183–2197.
30. Cermak, J.; Bendix, J. Detecting ground fog from space—A microphysics-based approach. *Int. J. Remote Sens.* **2011**, *32*, 3345–3371.
31. Egli, S.; Maier, F.; Bendix, J.; Thies, B. Vertical distribution of microphysical properties in radiation fogs—A case study. *Atmos. Res.* **2015**, *151*, 130–145.
32. Chiou, C.R.; Hsieh, C.F.; Wang, J.C.; Chen, M.Y.; Liu, H.Y.; Yeh, C.L.; Yang, S.-Z.; Chen, T.-Y.; Hsia, Y.-J.; Song, G.Z.M. The first national vegetation inventory in Taiwan. *Taiwan J. For. Sci.* **2009**, *24*, 295–302.
33. Yu, L.F.; Chen, Z.E.; Guo, T.H. Establishment of proper land-use assessment and management strategy for Deji Reservoir Catchment, Taiwan. *Water Air, Soil Pollution: Focus* **2009**, *9*, 323–338.
34. Klose, C. Climate and geomorphology in the uppermost geomorphic belts of the Central Mountain Range, Taiwan. *Quatern Int.* **2006**, *147*, 89–102.
35. Chen, C.S.; Chen, Y.L. The rainfall characteristics of Taiwan. *Mon. Weather Rev.* **2003**, *131*, 1323–1341.
36. Kao, S.C.; Kume, T.; Komatsu, H.; Liang, W.L. Spatial and temporal variations in rainfall characteristics in mountainous and lowland areas in Taiwan. *Hydrol Process* **2013**, *27*, 2651–2658.
37. Kerns, J.B.W.; Chen, Y.L.; Chang, M.Y. The diurnal cycle of winds, rain, and clouds over Taiwan during the Mei-Yu, summer, and autumn rainfall regimes. *Mon. Weather Rev.* **2010**, *138*, 497–516.
38. Taiwan Forestry Bureau. Available online: www.forest.gov.tw (accessed on 20 October 2014).
39. Lin, C.W.; Tseng, C.M.; Tseng, Y.H.; Fei, L.Y.; Hsieh, Y.C.; Tarolli, P. Recognition of large scale deep-seated landslides in forest areas of Taiwan using high resolution topography. *J. Asian Earth Sci.* **2013**, *62*, 389–400.
40. Lee, M.F.; Lin, T.C.; Vadeboncoeur, M.A.; Hwong, J.L. Remote sensing assessment of forest damage in relation to the 1996 strong typhoon Herb at Lienhuachi Experimental Forest, Taiwan. *Forest Ecol. Manag.* **2008**, *255*, 3297–3306.
41. Mabry, C.M.; Hamburg, S.P.; Lin, T.C.; Horng, F.W.; King, H.B.; Hsia, Y.J. Typhoon disturbance and stand-level damage patterns at a subtropical forest in Taiwan. *Biotropica* **1998**, *30*, 238–250.
42. Suzuki, T. *Forest Vegetation of East Asia*; Kokin-Shoin: Tokyo, Japan, 1952. (In Japanese)
43. Kira, T. *A New Classification of Climate in Eastern Asia as the Basis for Agricultural Geography*; Horticultural Institute Kyoto University: Kyoto, Japan, 1945.

44. Hijmans, R.J.; Cameron, S.E.; Parra, J.L.; Jones, P.G.; Jarvis, A. Very high resolution interpolated climate surfaces for global land areas. *Int. J. Climatol.* **2005**, *25*, 1965–1978.
45. Fawcett, T. An introduction to ROC analysis. *Pattern Recogn. Lett.* **2006**, *27*, 861–874.
46. Sing, T.; Sander, O.; Beerenwinkel, N.; Lengauer, T. ROCR: Visualizing classifier performance in R. *Bioinformatics* **2005**, *21*, 3940–3941.
47. Chen, C.S.; Huang, J.M. A numerical study of precipitation characteristics over Taiwan Island during the winter season. *Meteorol. Atmos. Phys.* **1999**, *70*, 167–183.
48. Chen, T.C.; Yen, M.C.; Huang, W.R.; Gallus, W.A., Jr. An East Asian cold surge: Case study. *Mon. Weather Rev.* **2002**, *130*, 2271–2290.
49. Liou, Y.A.; Kar, S.K. Study of cloud-to-ground lightning and precipitation and their seasonal and geographical characteristics over Taiwan. *Atmos. Res.* **2010**, *95*, 115–122.
50. Shieh, S.L.; Wang, S.T.; Cheng, M.D.; Yeh, T.C. *Tropical Cyclone Tracks over Taiwan from 1897 to 1996 and Their Applications*; Central Weather Bureau Tech. Rep. CWB86-1M-01; Central Weather Bureau: Taipei, Taiwan, 1998.
51. Tao, W.K.; Chen, C.S.; Jia, Y.; Lang, S. Two heavy precipitation events in Taiwan: Regional scale model simulations. In Proceedings of Workshop on Numerical Simulations of Precipitation in Taiwan Area, Chung-Li, Taiwan, 17–18 February 2000; pp. 19–20.
52. Boyle, J.S.; Chen, T.J. Synoptic aspects of the wintertime East Asian monsoon. In *Monsoon Meteorology*; Chang, C.P., Krishnamurti, T.N., Eds.; Oxford University Press: Oxford, UK, 1987; pp. 125–160.
53. Yeh, H.C.; Chen, Y.L. Characteristics of rainfall distributions over Taiwan during the Taiwan Area Mesoscale Experiment (TAMEX). *J. Appl. Meteorol.* **1998**, *37*, 1457–1469.
54. Chen, Y.L. Effects of island induced airflow on rainfall distributions during the Mei-Yu season over Taiwan. In Proceedings of Workshop on Numerical Simulations of Precipitation in Taiwan Area, Chung-Li, Taiwan, 17–18 February 2000; pp. 5–11.
55. Aldrich, M.; Billington, C.; Edwards, M.; Laidlaw, R. *A Global Directory of Tropical Montane Cloud Forests*; UNEP–WCMC: Cambridge, UK, 1997.
56. Lai, Y.J.; Chou, M.D.; Lin, P.H. Parameterization of topographic effect on surface solar radiation. *J. Geophys. Res.: Atmos.* **2010**, *115*, doi: 10.1029/2009JD012305.
57. Lai, Y.J.; Li, C.F.; Lin, P.H.; Wey, T.H.; Chang, C.S. Comparison of MODIS land surface temperature and ground-based observed air temperature in complex topography. *Int. J. Remote Sens.* **2012**, *33*, 7685–7702.
58. Schulz, H.M.; Thies, B.; Cermak, J.; Bendix, J. 1 km fog and low stratus detection using pan-sharpened MSG SEVIRI data. *Atmos. Meas. Tech.* **2012**, *5*, 2469–2480.